

Evidence for Muon Neutrino Oscillation in an Accelerator-Based Experiment

E. Aliu,¹ S. Andringa,¹ S. Aoki,¹⁰ J. Argyriades,³ K. Asakura,¹⁰ R. Ashie,³⁰ H. Berns,³³ H. Bhang,²⁰ A. Blondel,²⁶ S. Borghi,²⁶ J. Bouchez,³ J. Burguet-Castell,³² D. Casper,²⁸ C. Cavata,³ A. Cervera,²⁶ K. O. Cho,⁴ J. H. Choi,⁴ U. Dore,¹⁹ X. Espinal,¹ M. Fechner,³ E. Fernandez,¹ Y. Fukuda,¹⁵ J. Gomez-Cadenas,³² R. Gran,³³ T. Hara,¹⁰ M. Hasegawa,¹² T. Hasegawa,²² K. Hayashi,¹² Y. Hayato,⁷ R. L. Helmer,²⁵ J. Hill,²³ K. Hiraide,¹² J. Hosaka,³⁰ A. K. Ichikawa,⁷ M. Iinuma,⁸ A. Ikeda,¹⁷ T. Inagaki,¹² T. Ishida,⁷ K. Ishihara,³⁰ T. Ishii,⁷ M. Ishitsuka,³¹ Y. Itow,³⁰ T. Iwashita,⁷ H. I. Jang,⁴ E. J. Jeon,²⁰ I. S. Jeong,⁴ K. Joo,²⁰ G. Jover,¹ C. K. Jung,²³ T. Kajita,³¹ J. Kameda,³⁰ K. Kaneyuki,³¹ I. Kato,¹² E. Kearns,² D. Kerr,²³ C. O. Kim,¹¹ M. Khabibullin,⁹ A. Khotjantsev,⁹ D. Kielczewska,^{34,21} J. Y. Kim,⁴ S. Kim,²⁰ P. Kitching,²⁵ K. Kobayashi,²³ T. Kobayashi,⁷ A. Konaka,²⁵ Y. Koshio,³⁰ W. Kropp,²⁸ J. Kubota,¹² Yu. Kudenko,⁹ Y. Kuno,¹⁸ T. Kutter,^{27,13} J. Learned,²⁹ S. Likhoded,² I. T. Lim,⁴ P. F. Loverre,¹⁹ L. Ludovici,¹⁹ H. Maesaka,¹² J. Mallet,³ C. Mariani,¹⁹ T. Maruyama,⁷ S. Matsuno,²⁹ V. Matveev,⁹ C. Mauger,²¹ K. McConnel,¹⁴ C. McGrew,²³ S. Mikheyev,⁹ A. Minamino,³⁰ S. Mine,²⁸ O. Mineev,⁹ C. Mitsuda,³⁰ M. Miura,³⁰ Y. Moriguchi,¹⁰ T. Morita,¹² S. Moriyama,³⁰ T. Nakadaira,¹² M. Nakahata,³⁰ K. Nakamura,⁷ I. Nakano,¹⁷ T. Nakaya,¹² S. Nakayama,³¹ T. Namba,³⁰ R. Nambu,³⁰ S. Nawang,⁸ K. Nishikawa,¹² K. Nitta,⁷ F. Nova,¹ P. Novella,³² Y. Obayashi,³⁰ A. Okada,³¹ K. Okumura,³¹ S. M. Oser,²⁷ Y. Oyama,⁷ M. Y. Pac,⁵ F. Pierre,³ A. Rodriguez,¹ C. Saji,³¹ M. Sakuda,^{7,17} F. Sanchez,¹ A. Sarrat,²³ T. Sasaki,¹² K. Scholberg,^{6,14} R. Schroeter,²⁶ M. Sekiguchi,¹⁰ E. Sharkey,²³ M. Shiozawa,³⁰ K. Shiraishi,³³ G. Sitjes,³² M. Smy,²⁸ H. Sobel,²⁸ J. Stone,² L. Sulak,² A. Suzuki,¹⁰ Y. Suzuki,³⁰ T. Takahashi,⁸ Y. Takenaga,³¹ Y. Takeuchi,³⁰ K. Taki,³⁰ Y. Takubo,¹⁸ N. Tamura,¹⁶ M. Tanaka,⁷ R. Terri,²³ S. T'Jampens,³ A. Tornero-Lopez,³² Y. Totsuka,⁷ S. Ueda,¹² M. Vagins,²⁸ C. W. Walter,⁶ W. Wang,² R. J. Wilkes,³³ S. Yamada,⁹ S. Yamamoto,¹² C. Yanagisawa,²³ N. Yershov,⁹ H. Yokoyama,²⁴ M. Yokoyama,¹² J. Yoo,²⁰ M. Yoshida,¹⁸ and J. Zalipska²¹

(The K2K Collaboration)

¹*Institut de Fisica d'Altes Energies, Universitat Autònoma de Barcelona, E-08193 Bellaterra (Barcelona), Spain*

²*Department of Physics, Boston University, Boston, Massachusetts 02215, USA*

³*DAPNIA, CEA Saclay, 91191 Gif-sur-Yvette Cedex, France*

⁴*Department of Physics, Chonnam National University, Kwangju 500-757, Korea*

⁵*Department of Physics, Dongshin University, Naju 520-714, Korea*

⁶*Department of Physics, Duke University, Durham, North Carolina 27708, USA*

⁷*High Energy Accelerator Research Organization (KEK), Tsukuba, Ibaraki 305-0801, Japan*

⁸*Graduate School of Advanced Sciences of Matter, Hiroshima University, Higashi-Hiroshima, Hiroshima 739-8530, Japan*

⁹*Institute for Nuclear Research, Moscow 117312, Russia*

¹⁰*Kobe University, Kobe, Hyogo 657-8501, Japan*

¹¹*Department of Physics, Korea University, Seoul 136-701, Korea*

¹²*Department of Physics, Kyoto University, Kyoto 606-8502, Japan*

¹³*Department of Physics and Astronomy, Louisiana State University, Baton Rouge, Louisiana 70803-4001, USA*

¹⁴*Department of Physics, Massachusetts Institute of Technology, Cambridge, Massachusetts 02139, USA*

¹⁵*Department of Physics, Miyagi University of Education, Sendai 980-0845, Japan*

¹⁶*Department of Physics, Niigata University, Niigata, Niigata 950-2181, Japan*

¹⁷*Department of Physics, Okayama University, Okayama, Okayama 700-8530, Japan*

¹⁸*Department of Physics, Osaka University, Toyonaka, Osaka 560-0043, Japan*

¹⁹*University of Rome La Sapienza and INFN, I-000185 Rome, Italy*

²⁰*Department of Physics, Seoul National University, Seoul 151-747, Korea*

²¹*A. Soltan Institute for Nuclear Studies, 00-681 Warsaw, Poland*

²²*Research Center for Neutrino Science, Tohoku University, Sendai, Miyagi 980-8578, Japan*

²³*Department of Physics and Astronomy, State University of New York, Stony Brook, New York 11794-3800, USA*

²⁴*Department of Physics, Tokyo University of Science, Noda, Chiba 278-0022, Japan*

²⁵*TRIUMF, Vancouver, British Columbia, V6T 2A3, Canada*

²⁶*DPNC, Section de Physique, University of Geneva, CH1211, Geneva 4, Switzerland*

²⁷*Department of Physics & Astronomy, University of British Columbia, Vancouver, British Columbia, V6T 1Z1, Canada*

²⁸*Department of Physics and Astronomy, University of California, Irvine, California 92697-4575, USA*

²⁹*Department of Physics and Astronomy, University of Hawaii, Honolulu, Hawaii 96822, USA*

³⁰*Kamioka Observatory, Institute for Cosmic Ray Research, University of Tokyo, Kamioka, Gifu 506-1205, Japan*

³¹*Research Center for Cosmic Neutrinos, Institute for Cosmic Ray Research, University of Tokyo, Kashiwa, Chiba 277-8582, Japan*

³²*Instituto de Física Corpuscular, E-46071 Valencia, Spain*³³*Department of Physics, University of Washington, Seattle, Washington 98195-1560, USA*³⁴*Institute of Experimental Physics, Warsaw University, 00-681 Warsaw, Poland*

(Received 9 November 2004; published 3 March 2005)

We present results for ν_μ oscillation in the KEK to Kamioka (K2K) long-baseline neutrino oscillation experiment. K2K uses an accelerator-produced ν_μ beam with a mean energy of 1.3 GeV directed at the Super-Kamiokande detector. We observed the energy-dependent disappearance of ν_μ , which we presume have oscillated to ν_τ . The probability that we would observe these results if there is no neutrino oscillation is 0.0050% (4.0σ).

DOI: 10.1103/PhysRevLett.94.081802

PACS numbers: 14.60.Pq, 13.15.+g, 25.30.Pt, 95.55.Vj

Recent atmospheric [1–3], reactor [4], and solar neutrino [5,6] experiments show that the existence of neutrino oscillation and nonzero neutrino mass are very likely. Measurements of atmospheric neutrino suggest ν_μ to ν_τ oscillation with a mass squared difference (Δm^2) around 2.5×10^{-3} eV² and a mixing angle parameter ($\sin^2 2\theta$) that is almost unity [1,7].

The KEK (High Energy Accelerator Research Organization) to Kamioka long-baseline neutrino oscillation experiment (K2K) [8,9] is the first accelerator-based project to explore neutrino oscillation in the same Δm^2 region as atmospheric neutrinos. The neutrino beam is 98% ν_μ , whose direction is monitored every beam spill by measuring the profile of muons from the pion decays. The neutrino beam energy spectrum and profile are measured by the near neutrino detectors located 300 m from the production target. They consist of two detector sets: a 1 kiloton water Cherenkov detector (1KT) and a fine grained detector system. The far detector is Super-Kamiokande (SK), a 50 kt water Cherenkov detector, located 250 km from KEK.

In this Letter, we present evidence for the energy-dependent disappearance of ν_μ , which are presumed to have oscillated to ν_τ . We observe a distortion of the neutrino energy (E_ν) spectrum and a deficit in the total number of events. The expectation for these are derived from measurements at the near detectors and transformed using the energy-dependent ratio of the ν_μ flux at the far and near detectors (F/N ratio). This ratio accounts for the difference between the small portion of the beam near the center seen by SK and the large section of the beam seen by the near detectors. This is calculated using the neutrino beam Monte Carlo (MC) simulation and confirmed by measurements of pions from the target [8,9].

Data sample.—We have analyzed data taken from June 1999 to February 2004, which corresponds to 8.9×10^{19} protons on target (POT). From 1999 to 2001 (called K2K-I and SK-I), the inner detector surface of SK had 11 146 20-in. photomultiplier tubes (PMTs) covering 40% of the total area [10]. The fine grained detector system was comprised of a scintillating fiber and water detector (SciFi) [11], a lead glass calorimeter, and a muon range detector (MRD) [12]. Starting from January 2003 (K2K-II and SK-

II), 19% of the SK inner detector is covered using 5182 PMTs, each enclosed in a fiber reinforced plastic shell with an acrylic cover. The transparency and reflection of these covers in water are 97% and 1%, respectively. The near detector data from this period include 2.3×10^{19} POT without the lead glass (K2K-IIa), and then 1.9×10^{19} POT (K2K-IIb) with a fully active scintillator detector (SciBar) [13] in its place. Adding the K2K-II data doubles the statistics compared to the previous analysis [9].

The neutrino beam direction is monitored using neutrino events in the MRD. It is stable, within 1 mrad throughout the entire experimental period. Also, these events confirm that the energy spectrum is stable.

The 1KT data alone are used to estimate the expected total number of events at SK because the 1KT uses the same water target and the uncertainties in the neutrino cross section cancel. The event selection and the 25 ton fiducial volume are the same as in [9]. We select the subset of events in which all the energy is deposited in the inner detector (fully contained) and only one, muonlike Cherenkov ring is reconstructed (1-ring μ -like events) to estimate the E_ν spectrum along with data from the other near detectors. For these events, we reconstruct E_ν by using the measured muon momentum (p_μ) and direction (θ_μ). For the energy spectrum measurement, the largest contribution to the systematic uncertainty is $+2\%/ - 3\%$ in the overall energy scale.

The SciFi detector is made of layers of scintillating fibers between aluminum tanks filled with water. The fiducial mass is 5.6 tons. The K2K-I analysis includes events which reach the MRD and also events in which the muon track stops in the lead glass, with momentum as low as 400 MeV/ c , significantly lowering the energy threshold compared to [9]. The muon momentum threshold for K2K-IIa is 550 MeV/ c because in this case we restrict our analysis to events which have hit at least two layers in the MRD to improve the purity of muons.

The SciBar detector consists of 14 848 extruded scintillator strips read out by wavelength shifting fibers and multianode PMTs. Strips with dimensions of $1.3 \times 2.5 \times 300$ cm³ are arranged in 64 layers. Each layer consists of two planes to measure horizontal and vertical positions. The scintillator also acts as the neutrino interaction target; it is a fully active detector and has high efficiency for low

TABLE I. The reconstruction efficiency (%) and purity [in parentheses (%)] for the quasielastic interaction in each sub-sample estimated by MC simulation.

	1-track or 1-ring μ like	2-track		Total
		QE	non-QE	
1KT	53 (59)	53
SciFi I	39 (50)	5 (53)	2 (11)	46
SciFi IIa	36 (57)	5 (58)	2 (12)	42
SciBar	51 (57)	15 (72)	4 (17)	70
SK	86 (58)	86

momentum particles. Although the target is not water, possible differences due to nuclear effects are included in the systematic uncertainty.

In SciBar, tracks which traverse at least three layers (~ 8 cm) are reconstructed. The reconstruction efficiency for an isolated track longer than 10 cm is 99%. In the present analysis, we select charged current (CC) events by requiring that at least one of the tracks start from the 9.38 ton fiducial volume and extend to the MRD. With this requirement, the p_μ threshold is 450 MeV/c. The p_μ scale uncertainty, p_μ resolution, and θ_μ resolution are 2.7%, 80 MeV/c, and 1.6°, respectively. The efficiency for a second, short track is lower than that for a muon track mainly due to the overlap with the primary track. This efficiency smoothly increases from the threshold (8 cm, corresponding to a 450 MeV/c proton) and reaches 90% at 30 cm (670 MeV/c for proton).

For SciFi and SciBar, we select events in which one or two tracks are reconstructed. For two-track events, we use kinematic information to discriminate between quasielastic (QE) and non-QE interactions. The direction of the recoil proton can be predicted from p_μ and θ_μ assuming a QE interaction. If the difference between the observed and the predicted direction of the second track is within 25°, the event is in the QE enriched sample. Events for which this difference is more than 30° (25°) for SciFi (SciBar) are put into the non-QE sample. The QE efficiency and purity of the samples are estimated from the MC simulation and are summarized in Table I.

Near detector spectrum.—We measure the E_ν spectrum at the near detectors by fitting the two-dimensional distributions of p_μ versus θ_μ with a baseline MC expectation [9]. We simultaneously obtain the cross section ratio of non-QE to QE interactions (R_{nqe}) relative to our MC simulation. However, we observe a significant deficit of forward going muons in all near detector data compared to the MC. To avoid a bias due to this, we perform the E_ν fit using only data with $\theta_\mu > 20(10)^\circ$ for 1KT (SciFi and SciBar). The χ^2 value at the best fit is 538.5 for 479 degrees of freedom (DOF). The resulting E_ν spectrum and its error are summarized in Table II, while the best fit value of R_{nqe} is 0.95.

TABLE II. The E_ν spectrum fit results. Φ_{ND} is the best fit value of relative flux for each E_ν bin to the 1.0–1.5 GeV bin. The percentages of uncertainties in Φ_{ND} , F/N ratio, and reconstruction efficiencies of SK-I and SK-II are also shown.

E_ν (GeV)	Φ_{ND}	$\Delta(\Phi_{\text{ND}})$	$\Delta(F/N)$	$\Delta(\epsilon_{\text{SK-I}})$	$\Delta(\epsilon_{\text{SK-II}})$
0.0–0.5	0.032	46	2.6	3.7	4.5
0.5–0.75	0.32	8.5	4.3	3.0	3.2
0.75–1.0	0.73	5.8	4.3	3.0	3.2
1.0–1.5	$\equiv 1$...	4.9	3.3	8.2
1.5–2.0	0.69	4.9	10	4.9	7.8
2.0–2.5	0.34	6.0	11	4.9	7.4
2.5–3.0	0.12	13	12	4.9	7.4
3.0–	0.049	17	12	4.9	7.4

Muons in the forward direction also correspond to events with a low value for the square of the momentum transfer (q^2), the relevant parameter in the neutrino interaction models. From inspection of all subsamples, the amount of resonant pion production and coherent pion production at low q^2 in the MC simulation are possible sources of the forward muon deficit. In our MC, we use the model for resonant pion by Rein and Sehgal [14] with axial vector mass of 1.1 GeV/c². For coherent pion, we use the model by Rein and Sehgal [15] with the cross section calculated by Marteau *et al.* [16]. Figure 1 shows the q^2 distributions calculated from p_μ and θ_μ assuming CC-QE kinematics (q_{rec}^2). We modify the MC simulation used in the near and the far detector analysis to account for the effect of the observed deficit. For resonant pions, we suppress the cross section by q^2/A for $q^2 < A$ and leave it unchanged for $q^2 > A$. From a fit to the SciBar 2-track non-QE sample, A is 0.10 ± 0.03 (GeV/c²). Alternatively, if we assume that the source of the low q^2 deficit is coherent pion production, we find the observed distribution is reproduced best with zero coherent pion.

Considering both possibilities mentioned above, we fit the parameter R_{nqe} again and check the agreement with the data. The E_ν spectrum is kept fixed at the values already obtained in the first step, but now we use data at all angles. The best fit value for R_{nqe} is 1.02 (1.06) with χ^2/DOF of

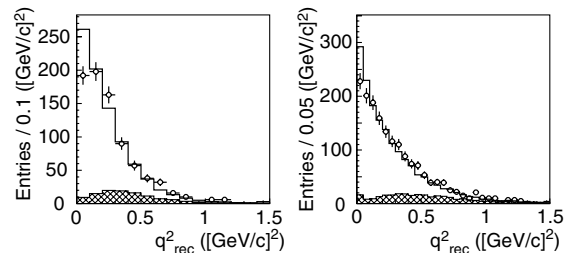


FIG. 1. The q_{rec}^2 distributions for 2-track non-QE samples of SciFi (left) and SciBar (right). Open circles, solid lines, and hatched areas show data, MC predictions, and the CC-QE component estimated from MC simulation, respectively.

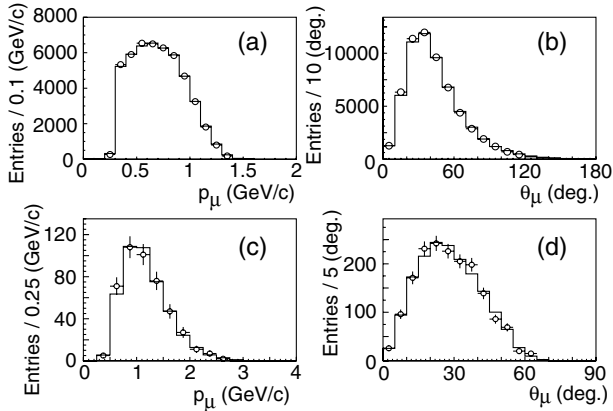


FIG. 2. A selection of muon momentum (p_μ) and direction (θ_μ) distributions: (a) the p_μ distribution of the 1KT fully contained 1-ring μ -like sample, (b) 1KT θ_μ for the same sample, (c) SciFi p_μ for the 2-track QE sample, and (d) SciBar θ_μ for the 2-track non-QE sample. Open circles represent data, while histograms are MC predictions using the best fit E_ν spectrum and suppression of the resonant pion production.

638.1/609 (667.1/606) when we suppress the resonant pion (eliminate the coherent pion). The p_μ and θ_μ distributions from all detectors are well reproduced for both cases with reasonable χ^2 , as shown in Fig. 2. If we repeat the fit with the E_ν spectrum free, the results are still consistent with the first step. Examining these results carefully, we conclude that we cannot identify which is the source of the observed deficit in the low q^2 region. Because the value of R_{nqe} changes depending on the choice of model, an additional systematic error of 0.1 is assigned to R_{nqe} . For the oscillation analysis presented in this Letter, we choose to suppress the resonance production mode in the MC simulation and when we determine the central value of R_{nqe} . However, we find that the final oscillation results and allowed regions do not change if we instead choose to eliminate coherent pion or use our MC without any corrections.

Oscillation analysis.—Events in SK from the accelerator are selected based on timing information from the global positioning system. The background coming from atmospheric neutrinos is estimated to be 2×10^{-3} events. For K2K – I + II there are 107 events in the 22.5 kt fiducial volume that are fully contained, have no energy seen in the outer detector, and have at least 30 MeV deposited in the inner detector. The expected number of fully contained events at SK without oscillation is $151^{+12}_{-10}(\text{syst})$. The major contributions to the errors come from the uncertainties in the far to near ratio (5.1%) and the normalization (5.1%); the latter is dominated by the uncertainty in the fiducial volumes due to the vertex reconstruction at both 1KT and SK.

We reconstruct the neutrino energy (E_μ^{rec}), assuming CC-QE kinematics, from p_μ and θ_μ for the 57 events in the 1-ring μ -like subset of the SK data. With these we measure the energy spectrum distortion caused by neutrino oscillation. The detector systematics of SK-I and SK-II are slightly different because of the change in the number of inner detector PMTs. In the oscillation analysis based on the energy spectrum, the main contribution to the systematic error is the energy scale uncertainty: 2.0% for SK-I and 2.1% for SK-II. Uncertainties for the ring counting and particle identification are estimated using the atmospheric neutrino data sample and MC simulation. The differences between the K2K and atmospheric neutrino fluxes are also taken into account.

A two-flavor neutrino oscillation analysis, with ν_μ disappearance, is performed using a maximum-likelihood method. The oscillation parameters, ($\sin^2 2\theta$, Δm^2), are estimated by maximizing the product of the likelihood for the observed number of fully contained events (\mathcal{L}_{num}) and that for the shape of the E_ν^{rec} spectrum ($\mathcal{L}_{\text{shape}}$). The probability density function (PDF) for \mathcal{L}_{num} is the Poisson probability for the expected number of events. The PDF for $\mathcal{L}_{\text{shape}}$ is the expected E_ν^{rec} distribution at SK, which is estimated from the MC simulation. The PDFs are defined for K2K-I and K2K-II separately. The systematic uncertainties due to the following sources are taken into account in the PDFs: the E_ν spectrum measured by the near detectors, the far to near ratio, the reconstruction efficiency and absolute energy scale of SK, the ratio of neutral current to charged current QE cross section, the ratio of CC non-QE to CC-QE cross section, and the overall normalization. The systematic uncertainties modify the expected distributions, and each is assumed to follow a Gaussian distribution [7]. A constraint term ($\mathcal{L}_{\text{syst}}$) is multiplied with the likelihood for each of these systematics, and $\mathcal{L}_{\text{num}} \times \mathcal{L}_{\text{shape}} \times \mathcal{L}_{\text{syst}}$ is maximized during the fit. The total number of parameters varied in the fit is 34.

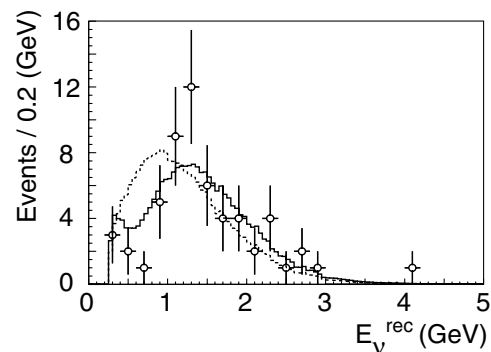


FIG. 3. The reconstructed E_ν distribution for the SK 1-ring μ -like sample. Points with error bars are data. The solid line is the best fit spectrum. The dashed line is the expected spectrum without oscillation. These histograms are normalized by the number of events observed (57).

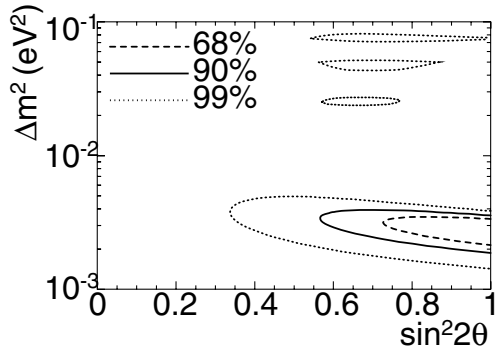


FIG. 4. Allowed regions of oscillation parameters. Dashed, solid, and dot-dashed lines are 68.4%, 90% and 99% C.L. contours, respectively.

The best fit point within the physical region is $(\sin^2 2\theta, \Delta m^2) = (1.0, 2.8 \times 10^{-3} \text{ eV}^2)$. The expected number of events at this point is 103.8, which agrees well with the 107 observed. The best fit E_ν distribution is shown with the data in Fig. 3. The consistency between the observed and fit E_ν distributions is checked using a Kolmogorov-Smirnov (KS) test. For the best fit parameters, the KS probability is 36%, while that for the no-oscillation hypothesis is 0.08%. The highest likelihood is at a point $(1.5, 2.2 \times 10^{-3} \text{ eV}^2)$ which is outside of the physical region. The probability that we would get $\sin^2 2\theta \geq 1.5$ if the true parameters are our best fit physical parameters is 13%, based on MC virtual experiments. For the rest of this Letter we refer only to the physical region best fit. The fit results for all the systematic parameters are reasonable. The fits for the K2K-I and K2K-II subsamples are consistent with the result for the whole sample.

The possibility that the observations are due to a statistical fluctuation instead of neutrino oscillation is estimated by computing the likelihood ratio of the no-oscillation case to the best fit point. If there is no oscillation, the probability of this result is 0.0050% (4.0σ). When only normalization (shape) information is used, the probability is 0.26% (0.74%). Allowed regions for the oscillation parameters are evaluated by calculating the likelihood ratio of each point to the best fit point and are drawn in Fig. 4. The 90% C.L. contour crosses the $\sin^2 2\theta = 1$ axis at $\Delta m^2 = 1.9$ and $3.6 \times 10^{-3} \text{ eV}^2$. The oscillation parameters from the E_ν spectrum distortion alone, or the total event analysis alone, also agree.

In conclusion, using accelerator-produced neutrinos, we see the same neutrino oscillation discovered with atmospheric neutrino measurements. This result is based on data from 1999 to 2004, a total of 8.9×10^{19} POT. The observed number of events and energy spectrum of neutrinos at SK are consistent with neutrino oscillation. The probability that we would see this result if there is no oscillation

is 0.0050% (4.0σ). The allowed regions of the oscillation parameters from the K2K experiment are consistent with the atmospheric neutrino measurements.

We thank the KEK and ICRR directorates for their strong support and encouragement. K2K is made possible by the inventiveness and the diligent efforts of the KEK-PS Machine Group and Beam Channel Group. We gratefully acknowledge the cooperation of the Kamioka Mining and Smelting Company. This work has been supported by the Ministry of Education, Culture, Sports, Science and Technology of the Government of Japan, the Japan Society for Promotion of Science, the U.S. Department of Energy, the Korea Research Foundation, the Korea Science and Engineering Foundation, NSERC Canada and Canada Foundation for Innovation, the Istituto Nazionale di Fisica Nucleare (Italy), the Spanish Ministry of Science and Technology, and Polish KBN Grants No. 1P03B08227 and No. 1P03B03826.

-
- [1] Super-Kamiokande Collaboration, Y. Ashie *et al.*, Phys. Rev. Lett. **93**, 101801 (2004).
 - [2] MACRO Collaboration, M. Ambrosio *et al.*, Phys. Lett. B **566**, 35 (2003).
 - [3] Soudan2 Collaboration, M. Sanchez *et al.*, Phys. Rev. D **68**, 113004 (2003).
 - [4] KamLAND Collaboration, T. Araki *et al.*, Phys. Rev. Lett. (to be published).
 - [5] Super-Kamiokande Collaboration, M. B. Smy *et al.*, Phys. Rev. D **69**, 011104 (2004).
 - [6] SNO Collaboration, S. N. Ahmed *et al.*, Phys. Rev. Lett. **92**, 181301 (2004).
 - [7] Super-Kamiokande Collaboration, Y. Fukuda *et al.*, Phys. Rev. Lett. **81**, 1562 (1998).
 - [8] K2K Collaboration, S. H. Ahn *et al.*, Phys. Lett. B **511**, 178 (2001).
 - [9] K2K Collaboration, M. H. Ahn *et al.*, Phys. Rev. Lett. **90**, 041801 (2003).
 - [10] Super-Kamiokande Collaboration, S. Fukuda *et al.*, Nucl. Instrum. Methods Phys. Res., Sect. A **501**, 418 (2003).
 - [11] K2K Collaboration, A. Suzuki *et al.*, Nucl. Instrum. Methods Phys. Res., Sect. A **453**, 165 (2000); B. J. Kim *et al.*, Nucl. Instrum. Methods Phys. Res., Sect. A **497**, 450 (2003).
 - [12] K2K MRD Group T. Ishii *et al.*, Nucl. Instrum. Methods Phys. Res., Sect. A **482**, 244 (2002); T. Ishii *et al.*, *ibid.* **488**, 673(E) (2002).
 - [13] K. Nitta *et al.*, Nucl. Instrum. Methods Phys. Res., Sect. A **535**, 147 (2004).
 - [14] D. Rein and L. M. Sehgal, Ann. Phys. (N.Y.) **133**, 79 (1981).
 - [15] D. Rein and L. M. Sehgal, Nucl. Phys. B **223**, 29 (1983).
 - [16] J. Marteau, J. Delorme, and M. Ericson, Nucl. Instrum. Methods Phys. Res., Sect. A **451**, 76 (2000).